

# Boosting vector leptoquark searches with boosted tops

Arvind Bhaskar,<sup>1,\*</sup> Tanumoy Mandal,<sup>2,†</sup> and Subhadip Mitra<sup>1,‡</sup>

<sup>1</sup>Center for Computational Natural Sciences and Bioinformatics,  
International Institute of Information Technology, Hyderabad 500 032, India

<sup>2</sup>Indian Institute of Science Education and Research Thiruvananthapuram, Vithura, Kerala, 695551, India

(Dated: April 3, 2020)

At the LHC, a TeV-scale leptoquark (LQ) that decays dominantly to a top quark ( $t$ ) and a light charged lepton ( $\ell = e, \mu$ ) would form a resonance system of *boosted- $t$  + high- $p_T$ - $\ell$* . We consider all possible vector LQ models within the Buchmüller-Rückl-Wyler classifications with the desired decay. We propose simple phenomenological Lagrangians that are suitable for bottom-up/experimental studies and, at the same time, can cover the relevant parameter spaces of these models. In this simplified framework, we study the pair and single production channels of vector LQs at the LHC. Interestingly, we find that, like the pair production, the cross sections of some single production processes also depend on the parameter  $\kappa$  that appears in the gluon-vector LQ coupling. We adopt a search strategy of selecting events with at least one boosted hadronic top quark and exactly two high- $p_T$  leptons of the same flavor and opposite sign. This combines events from the pair and single production processes and, therefore, can enhance the discovery potential than that of the pair-production-only searches. For  $5\sigma$  discovery we find that vector LQs can be probed up to 2.55 TeV for 100% branching ratio in the  $t\ell$  decay mode and  $\mathcal{O}(1)$  new couplings at the 14 TeV LHC with  $3 \text{ ab}^{-1}$  of integrated luminosity.

## I. INTRODUCTION

In the recent past, several experimental collaborations have reported some hints of lepton flavor universality violation in the heavy meson decays. Collectively, these point toward the existence of some physics beyond the Standard Model (SM) as the SM gauge interactions are flavor-blind. Intriguingly, these seem to be quite tenacious and have created a lot of excitement in the particle physics community. Initially, the BaBar collaboration found two significant anomalies in the flavor changing charged current decays of the  $B$ -meson via the  $b \rightarrow c\tau\nu$  transition. They reported the anomalies in terms of excesses in the  $R_{D^{(*)}}$  observables defined as the ratios of branching ratios (BRs) to reduce some systematic and hadronic uncertainties [1, 2]. Since then, the excesses have survived the later measurements by the LHCb [3–5] and Belle [6–9] collaborations. The statistical average of these two observables obtained in the  $R_D - R_{D^*}$  plane by the HFLAV group puts the anomalies away from the corresponding SM predictions [10–13] by a combined significance of  $\sim 3.1\sigma$ . The LHCb collaboration has also observed downward deviations of about  $2.5\sigma$  [14–18] from the SM predictions [19, 20] in the flavor changing neutral current transition  $b \rightarrow s\mu\mu$  measured in terms of the  $R_{K^{(*)}}$  observables. Similarly, an excess of about  $\sim 2\sigma$  is found in another observable  $R_{J/\psi}$  [21]. In addition, a long-standing discrepancy of about  $\sim 3.5\sigma$  exists in the muon anomalous magnetic moment measurement [22].

It is known that TeV-scale leptoquarks (LQs) are good candidates to address the flavor anomalies. Moreover, their phenomenology has been explored in various other contexts also [23–75]. LQs are color-triplet bosons [either scalars (sLQs) or vectors (vLQs)] predicted by many beyond the SM theories [76–80]. They have fractional electric charges and carry both lepton and baryon numbers. In general, a LQ can couple to a quark and a lepton of either the same or different generations. The flavor anomalies suggest that LQs couple

more strongly to the third generation fermions than the other two. Cross-generational couplings of LQs could generate flavor changing neutral currents – the ones involving the first and second generations are tightly constrained. However, bounds are relatively weaker when a fermion of third generation is involved.

Among the current LHC programs, the search for LQs is one of the important ones. Usually, the LHC searches are done for LQs that couple to quarks and leptons of the same generation and are labeled accordingly. For example, pair production of a scalar LQ that decays to a top quark and tau lepton (or a bottom quark and a tau lepton or neutrino), i.e, a third generation LQ, has been extensively analyzed by both the ATLAS [81, 82] and the CMS [83, 84] collaborations. Altogether, the current bound on the third generation LQ is roughly about a TeV (this, of course, depends on various assumptions and we refer the reader to the actual papers for details). However, the flavor-motivated LQ models with sizable cross-generational couplings would have exotic signatures and require different search strategies. Of late, the nonstandard decay modes of LQs have started to gain attention; the CMS collaboration has published their first results on the pair production searches of LQs in the  $t\mu\mu$  channel [85]. Based on the 13 TeV data, they performed a prospect study for the pair production of sLQs in the  $t\mu\mu$  channel at the high-luminosity LHC (HL-LHC) [86].

Earlier in Ref [87], we investigated the HL-LHC prospects of sLQs that couple dominantly to the top quark in some detail. There, we focused on charge  $1/3$  and  $5/3$  sLQs that decay to a top quark and a charged lepton. Even though we considered only third generation quarks, interestingly, we found that in some scenarios single productions can improve their prospects significantly.<sup>1</sup> In this paper, we present a similar follow-up study for vLQs. Here too, we concentrate on a specific subset of possible vLQs that dominantly couple with a top quark and can decay to a top quark and a light charged lepton ( $e$  or

<sup>1</sup> This is interesting because, when a LQ (or any other particle) mostly couples to the third generation quarks, we generally expect their single productions to be ignorable as the bottom (top) quark density in proton is small (nonexistent) to play any significant role at the LHC.

\* arvind.bhaskar@research.iiit.ac.in

† tanumoy@iisertvm.ac.in

‡ subhadip.mitra@iiit.ac.in

$\mu$ ) with a substantial BR. Since, an analysis of the pair production of vLQs that decay to a top quark and a neutrino at the LHC is available from Ref. [88], in this paper we do not analyze this channel again. Instead, we present a set of simplified models that covers all the possibilities of a vLQ decaying to a top quark and any lepton. These are suitable for experimental analysis. We also demonstrate how they are related to the known models of vLQs [89, 90].

Our main motivation for considering this specific type of vLQs is to investigate their collider discovery/exclusion potential by making use of the boosted top signature coming from the LQ decay. They form an exotic resonance system with a boosted top and a high- $p_T$  lepton and provide a novel way to search for these models at the LHC. Various flavor anomalies suggest that cross-generational Yukawa-type LQ couplings with top and lepton might be large. A large coupling makes various single production channels important, especially in the high mass region. In our analysis, we adopt the same search strategy as the one we proposed for the sLQs [87]. We identify our signal by selecting at least one boosted hadronic top and exactly two high- $p_T$  leptons and demand the highest- $p_T$  top (if there are more than one tops) and one of the selected lepton to reconstruct a heavy system, i.e., the LQ. As we have demonstrated before [87, 91–93], such selection strategy combines pair and single production events and increase the LHC reach. Although, pair production is suitable for probing the low mass region, single production takes over when the LQ becomes heavy. Compared to the sLQs, the pair production cross sections for vLQs are relatively bigger and hence, the current mass limits obtained for the pair productions are generally higher for the vLQs than for the sLQs. In case for vLQs, the importance of single productions becomes visible for relatively higher mass compared to sLQs. We shall see that the discovery prospects of the vLQs at the HL-LHC is significantly improved if the new couplings controlling single productions are of order unity.

Before we proceed further, we note that since this is a follow-up paper of Ref. [87], we shall frequently refer to that paper and omit some details that are common while ensuring that our presentation is self-contained. The rest of the paper is organized as follows. In section II, we describe the vLQ models and introduce simplified models suitable for experimental analysis. In section III, we discuss the LHC phenomenology and illustrate our search strategy and then present our estimations in section IV. Finally, we summarize and conclude in section V.

## II. VECTOR LEPTOQUARK MODELS

To conserve electromagnetic charge, vLQs that decay to a top-lepton pair would have either electric charge equal to  $\pm 1/3$  or  $\pm 5/3$  (if the lepton is a charged one) or  $2/3$  (if lepton is a neutrino). This means that amongst the vLQs listed in Refs. [89, 90], the weak singlets  $U_1$  and  $\tilde{U}_1$ , doublets  $V_2$  and  $\tilde{V}_2$  and the triplet  $U_3$  would qualify for our study. Below, we display the relevant terms in the interaction Lagrangians following the notation of Ref. [90]. To avoid proton decay constraints, we ignore the diquark operators.

■  $\tilde{U}_1 = (\mathbf{3}, \mathbf{1}, 5/3)$ : The electric charge of  $\tilde{U}_1$  is  $5/3$ . Hence, it couples exclusively with the right-handed leptons:

$$\mathcal{L} \supset \tilde{x}_{1\ 3j}^{RR} \bar{u}_R^i \gamma^\mu \tilde{U}_{1,\mu} \ell_R^j + \text{H.c.}, \quad (1)$$

where  $u_R$  and  $\ell_R$  are an SM right-handed up-type quark and a charged lepton respectively and  $i, j = \{1, 2, 3\}$  are the generation indices. The color indices are suppressed. For our purpose, we consider only those terms that would connect vLQ to a third generation quark and ignore the rest,

$$\mathcal{L} \supset \tilde{x}_{1\ 3j}^{RR} \bar{t}_R (\gamma \cdot \tilde{U}_1) \ell_R^j + \text{H.c.} \quad (2)$$

■  $U_1 = (\mathbf{3}, \mathbf{1}, 2/3)$ : The necessary interaction terms for the charge  $2/3$   $U_1$  can be written as,

$$\mathcal{L} \supset x_{1\ ij}^{LL} \bar{Q}_L^i \gamma^\mu U_{1,\mu} L_L^j + x_{1\ ij}^{RR} \bar{d}_R^i \gamma^\mu U_{1,\mu} \ell_R^j + \text{H.c.}, \quad (3)$$

where  $Q_L$ ,  $L_L$  and  $d_R$  are the SM left-handed quark doublet, lepton doublet and a down-type right-handed quark, respectively. The  $i = 3$  terms can be written explicitly as,

$$\mathcal{L} \supset x_{1\ 3j}^{LL} \left\{ \bar{t}_L (\gamma \cdot U_1) \nu_L^j + \bar{b}_L (\gamma \cdot U_1) \ell_L^j \right\} + x_{1\ 3j}^{RR} \bar{b}_R (\gamma \cdot U_1) \ell_R^j + \text{H.c.} \quad (4)$$

■  $V_2 = (\bar{\mathbf{3}}, \mathbf{2}, 5/6)$ : For  $V_2$ , the Lagrangian is as follows,

$$\mathcal{L} \supset x_{2\ ij}^{RL} \bar{d}_R^i \gamma^\mu V_{2,\mu}^a \epsilon^{ab} L_L^j + x_{2\ ij}^{LR} \bar{Q}_L^{i,a} \gamma^\mu \epsilon^{ab} V_{2,\mu}^b \ell_R^j + \text{H.c.} \quad (5)$$

The superscript  $C$  denotes charge conjugation. Expanding the Lagrangian we get,

$$\mathcal{L} \supset -(x_{2\ ij}^{RL} \mathbf{U})_{ij} \bar{d}_R^i \gamma^\mu V_{2,\mu}^{1/3} \nu_L^j + x_{2\ ij}^{RL} \bar{d}_R^i \gamma^\mu V_{2,\mu}^{4/3} \ell_L^j + (\mathbf{V}^T x_{2\ ij}^{LR})_{ij} \bar{u}_L^i \gamma^\mu V_{2,\mu}^{1/3} \ell_R^j - x_{2\ ij}^{LR} \bar{d}_L^i \gamma^\mu V_{2,\mu}^{4/3} \ell_R^j + \text{H.c.}, \quad (6)$$

where  $\mathbf{U}$  and  $\mathbf{V}$  represent the Pontecorvo-Maki-Nakagawa-Sakata (PMNS) neutrino mixing matrix and the Cabibbo-Kobayashi-Maskawa (CKM) quark mixing matrix, respectively. We assume  $\mathbf{U}$  to be unity, as the LHC is blind to the flavor of the neutrinos. Similarly, since the small off-diagonal terms of the CKM matrix play negligible role at the LHC, we assume a diagonal CKM matrix for simplicity. Hence, the terms relevant for our analysis are,

$$\mathcal{L} \supset -x_{2\ 3j}^{RL} \bar{b}_R^i \left\{ (\gamma \cdot V_2^{1/3}) \nu_L^j - (\gamma \cdot V_2^{4/3}) \ell_L^j \right\} + x_{2\ 3j}^{LR} \left\{ \bar{t}_L^i (\gamma \cdot V_2^{1/3}) - \bar{b}_L^i (\gamma \cdot V_2^{4/3}) \right\} \ell_R^j + \text{H.c.} \quad (7)$$

■  $\tilde{V}_2 = (\bar{\mathbf{3}}, \mathbf{2}, -1/6)$ : For  $\tilde{V}_2$ , the Lagrangian becomes,

$$\mathcal{L} \supset \tilde{x}_{2\ ij}^{RL} \bar{u}_R^i \gamma^\mu \tilde{V}_{2,\mu}^b \epsilon^{ab} L_L^j + \text{H.c.} \quad (8)$$

Expanding it we get,

$$\mathcal{L} \supset -\tilde{x}_{2\ ij}^{RL} \bar{u}_R^i \gamma^\mu \tilde{V}_{2,\mu}^{1/3} \ell_L^j + (\tilde{x}_{2\ ij}^{RL} \mathbf{U})_{ij} \bar{u}_R^i \gamma^\mu \tilde{V}_{2,\mu}^{-2/3} \nu_L^j + \text{H.c.} \quad (9)$$

The terms with the third generation quarks are

$$\mathcal{L} \supset \tilde{x}_{2\ 3j}^{RL} \bar{t}_R^i \left\{ -(\gamma \cdot \tilde{V}_2^{1/3}) \ell_L^j + (\gamma \cdot \tilde{V}_2^{-2/3}) \nu_L^j \right\} + \text{H.c.} \quad (10)$$

■  $U_3 = (\mathbf{3}, \mathbf{3}, 2/3)$ : The necessary interaction terms for the triplet  $U_3$  are,

$$\mathcal{L} \supset x_{3\ ij}^{LL} \bar{Q}_L^{i,a} \gamma^\mu (\tau^k U_{3,\mu}^k)^{ab} L_L^{j,b} + \text{H.c.}, \quad (11)$$

Benchmark scenario	Possible charge(s)	Simplified models [Eqs. (14) – (16)]			LQ models [Eqs. (1) – (13)]			
		Type of LQ	Non-zero couplings equal to $\lambda$	Charged lepton chirality fraction	Type of LQ	Non-zero coupling equal to $\lambda$	Decay mode(s)	Branching ratios(s) $\{\beta, 1 - \beta\}$
LC	1/3	$\chi_1$	$\Lambda_\ell$	$\eta_L = 1$	$\tilde{V}_2^{1/3}$	$\tilde{x}_{2\ 3j}^{RL}$	$t\ell$	$\{100\%, 0\}$
	2/3	$\chi_2$	$\bar{\Lambda}_\nu$	—	$(\tilde{V}_2^{-2/3})^\dagger$	$(\tilde{x}_{2\ 3j}^{RL})^*$	$t\nu$	
	5/3	$\chi_5$	$\tilde{\Lambda}_\ell$	$\eta_L = 1$	$U_3^{5/3}$	$\sqrt{2} x_{3\ 3j}^{LL}$	$t\ell$	
LCSS*	2/3	$\chi_2$	$\bar{\Lambda}_\ell = \bar{\Lambda}_\nu$	$\eta_L = 1$	$U_1$	$x_{1\ 3j}^{LL}$	$\{t\nu, b\ell\}$	$\{50\%, 50\%\}$
LCOS			$\bar{\Lambda}_\ell = -\bar{\Lambda}_\nu$		$U_3^{2/3}$	$-x_{3\ 3j}^{LL}$		
RC	1/3	$\chi_1$	$\Lambda_\ell$	$\eta_R = 1$	$V_2^{1/3}$	$x_{2\ 3j}^{LR}$	$t\ell$	$\{100\%, 0\}$
	5/3	$\chi_5$	$\tilde{\Lambda}_\ell$		$\tilde{U}_1$	$\tilde{x}_{1\ 3j}^{RR}$		
RLCSS*	1/3	$\chi_1$	$\Lambda_\ell = \Lambda_\nu$	$\eta_R = 1$	$V_2^{1/3}$	$x_{2\ 3j}^{LR} = -x_{2\ 3j}^{RL}$	$\{t\ell, b\nu\}$	$\{50\%, 50\%\}$
RLCOS*			$\Lambda_\ell = -\Lambda_\nu$		$V_2^{1/3}$	$x_{2\ 3j}^{LR} = x_{2\ 3j}^{RL}$		

TABLE I. Summary of the nine benchmark scenarios considered. The branching ratio for a  $\chi$  to decay to a top-quark,  $\beta$  is fixed in any model [Eqs. (1) – (13)], except for  $U_1$  in the LCSS scenario ( $\beta \leq 50\%$ ) and for  $V_2^{1/3}$  in the RLCS/OS scenarios where  $0 \leq \beta < 100\%$  (for  $\beta = 100\%$ , these two scenarios become the same as the RC scenario). The exceptional scenarios are marked by an asterisk. Here,  $\lambda$  is a generic free coupling parameter. For simplicity, we have chosen only this one coupling to control all the non-zero new couplings in every benchmark. This essentially means choosing  $\beta$  to be 50% in the exceptional scenarios also.

where  $\tau^k$  denotes the Pauli matrices. This can be expanded as

$$\begin{aligned} \mathcal{L} \supset & -x_{ij}^{LL} \bar{d}_L^i \gamma^\mu U_\mu^{2/3} \ell_L^j + (\mathbf{V} x_3^{LL} \mathbf{U})_{ij} \bar{u}_L^i \gamma^\mu U_\mu^{2/3} \nu_L^j \\ & + \sqrt{2} (x_3^{LL} \mathbf{U})_{ij} \bar{d}_L^i \gamma^\mu U_\mu^{-1/3} \nu_L^j + \sqrt{2} (\mathbf{V} x_3^{LL})_{ij} \bar{u}_L^i \gamma^\mu U_\mu^{5/3} \ell_L^j \\ & + \text{H.c.} \end{aligned} \quad (12)$$

The terms for the third generation quarks can be written explicitly as,

$$\begin{aligned} \mathcal{L} \supset & x_{3\ 3j}^{LL} \left\{ -\bar{b}_L (\gamma \cdot U_3^{2/3}) \ell_L^j + \bar{t}_L (\gamma \cdot U_3^{2/3}) \nu_L^j \right. \\ & \left. + \sqrt{2} \bar{b}_L (\gamma \cdot U_3^{-1/3}) \nu_L^j + \sqrt{2} \bar{t}_L (\gamma \cdot U_3^{5/3}) \ell_L^j \right\} \\ & + \text{H.c.} \end{aligned} \quad (13)$$

### A. Simplified model and benchmark scenarios

The above models can be simplified into the following phenomenological Lagrangians,

$$\begin{aligned} \mathcal{L} \supset & \Lambda_\ell \left\{ \sqrt{\eta_R} \bar{t}_L^C (\gamma \cdot \chi_1) \ell_R + \sqrt{\eta_L} \bar{t}_R^C (\gamma \cdot \chi_1) \ell_L \right\} \\ & + \Lambda_\nu \bar{b}_R^C (\gamma \cdot \chi_1) \nu_L + \text{H.c.}, \end{aligned} \quad (14)$$

$$\begin{aligned} \mathcal{L} \supset & \bar{\Lambda}_\ell \left\{ \epsilon_R \sqrt{\eta_R} \bar{b}_R (\gamma \cdot \chi_2) \ell_R + \sqrt{\eta_L} \bar{b}_L (\gamma \cdot \chi_2) \ell_L \right\} \\ & + \bar{\Lambda}_\nu \bar{t}_L (\gamma \cdot \chi_2) \nu_L + \text{H.c.}, \end{aligned} \quad (15)$$

$$\begin{aligned} \mathcal{L} \supset & \bar{\Lambda}_\ell \left\{ \sqrt{\eta_R} \bar{t}_R (\gamma \cdot \chi_5) \ell_R + \sqrt{\eta_L} \bar{t}_L (\gamma \cdot \chi_5) \ell_L \right\} \\ & + \text{H.c.}, \end{aligned} \quad (16)$$

where we have suppressed the lepton generation index. We denote a generic charge  $\pm n/3$  vLQ by  $\chi_n$ . Here,  $\eta_L$  and  $\eta_R = 1 - \eta_L$  are the charged lepton chirality fractions [87, 92]. In Eq. (15), we have introduced a sign term,  $\epsilon_R = \pm 1$  to incorporate a possible relative sign between the left-handed and the right-handed terms [see Eq. (7)]. We shall consider only real couplings in our analysis for simplicity.

As we did for the sLQs [87], here also we identify some benchmark scenarios with the simplified models (see Table I).

Each scenario corresponds to one of the realizable models described above [see Eqs. (1) – (13)]. Here, we have ignored any possible mixing among the vLQs. The BR for a  $\chi$  to decay to a top-quark,  $\beta$  is fixed in any model [Eqs. (1) – (13)], except for two cases that we shall describe shortly. For simplicity, we choose only one free coupling  $\lambda$  parametrizing the non-zero new couplings in every benchmark scenario (see the fourth and seventh columns of Table. I. By doing this, we are essentially choosing  $\beta$  to be 50% in the free  $\beta$  scenarios also.)

- In the Left Coupling (LC) scenario, a  $\chi$  can directly couple with left-handed leptons. We set  $\lambda$  equal to  $\Lambda_\ell$  (for  $\chi_1$ ) or  $\tilde{\Lambda}_\ell$  (for  $\chi_5$ ) or  $\bar{\Lambda}_\nu$  (for  $\chi_2$ ) and put all other couplings to zero. For  $\chi_1$  and  $\chi_5$  we set  $\eta_L = 1$ . Here,  $\chi_1$  represents a  $\tilde{V}_2^{1/3}$  with  $\Lambda_\ell = \tilde{x}_{2\ 3j}^{RL}$ ,  $\chi_5$  represents a  $U_3^{5/3}$  with  $\tilde{\Lambda}_\ell = \sqrt{2} x_{3\ 3j}^{LL}$  and  $\chi_2$  represents an anti- $\tilde{V}_2^{-2/3}$  with  $\bar{\Lambda}_\nu = (\tilde{x}_{2\ 3j}^{RL})^*$ . In this scenario, a  $\chi_1$  or  $\chi_5$  decay to  $t\ell$  pairs and a  $\chi_2$  decays to  $t\nu$  pairs all the time.
- If a  $\chi_2$  is of  $U_1$  or  $U_3^{2/3}$  type, it can also decay to a  $b\ell$  pair. Hence, it is possible that a  $\chi_2$  couples with left-handed leptons but the BR for the  $\chi_2 \rightarrow t\nu$  ( $\beta$ ) is 50%. Such possibilities are captured in the Left Couplings with the Same Signs (LCSS) or the Left Couplings with Opposite Signs (LCOS) scenarios. The difference between these two comes from the different relative signs between the  $\chi_2 b\ell$  and  $\chi_2 t\nu$  couplings. In LCSS, the  $\chi_2$  behaves as a  $U_1$  with  $\bar{\Lambda}_\ell = \bar{\Lambda}_\nu = x_{1\ 3j}^{LL}$ , whereas in LCOS it behaves as a  $U_3^{2/3}$  with  $\bar{\Lambda}_\ell = -\bar{\Lambda}_\nu = -x_{3\ 3j}^{LL}$ . It is important to note that in the  $U_1$  case, it is possible to have  $\beta < 50\%$  if we consider a non-zero  $x_{1\ 3j}^{RR}$ . This can be seen from Eq. (4). Unlike the sLQ case [87], the LCSS and LCOS scenarios for the vLQ yield the same single production cross section as there is no interference among the contributing diagrams.
- The Right Coupling (RC) scenario, where a LQ couples only to right-handed charged leptons, is exclusive to  $\chi_1$  and  $\chi_5$ . Like the LC scenario, here we have  $\beta = 100\%$ . In this case a  $\chi_1$  behaves as a  $V_2^{1/3}$  with  $\Lambda_\ell = x_{2\ 3j}^{LR}$  and a  $\chi_5$  behaves as a  $\tilde{U}_1$  with  $\tilde{\Lambda}_\ell = x_{1\ 3j}^{RR}$ .

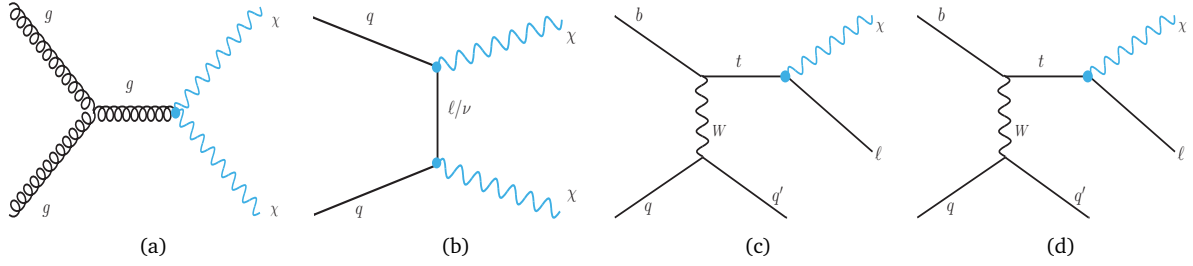


FIG. 1. Representative Feynman diagrams for the LQ production at the LHC. Diagrams (a) and (b) show pair production processes and (c) and (d) show single production processes.

- Unlike the sLQ  $\phi_1$  (see Ref. [87]), the  $\chi_1$  type vLQs (if it is  $V_2^{1/3}$ ) can decay to both  $t\ell$  and  $b\nu$  pairs, provided  $\Lambda_\ell$  and  $\Lambda_\nu$  both are nonzero. We design two scenarios, namely, Right (lepton) Left (neutrino) Couplings with the Same Signs (RLCSS) where  $\chi_1 \equiv V_2^{1/3}$  with  $\Lambda_\ell = \Lambda_\nu = x_2^{LR} = x_2^{RL}$  and Right (lepton) Left (neutrino) Couplings with Opposite Signs (RLCOS) where  $\chi_1 \equiv V_2^{1/3}$  with  $\Lambda_\ell = -\Lambda_\nu = x_2^{LR} = x_2^{RL}$ . In these two scenarios,  $\beta$  can be anything between zero and 100% as both involve two independent couplings [ $x_2^{LR}$  and  $x_2^{RL}$ , see Eq. (7)]. We, however, consider only  $\beta = 50\%$  for these benchmarks. We introduce these two benchmarks for completeness, though, for our purpose, these two are equivalent. As there is no interference contribution sensitive to this sign flip, all the production processes would have the same cross sections in both the scenarios.

Before we move on, we note that the kinetic terms for a vector leptoquark contains a free parameter, usually denoted as  $\kappa$  [90],

$$\mathcal{L} \supset -\frac{1}{2}\chi_{\mu\nu}^\dagger\chi^{\mu\nu} + M_\chi^2\chi_\mu^\dagger\chi^\mu - ig_s\kappa\chi_\mu^\dagger T^a\chi_\nu G^{a\mu\nu}, \quad (17)$$

where  $\chi_{\mu\nu}$  stands for the field strength tensor of  $\chi$ . This parameter  $\kappa$  can change pair and interestingly, some single production cross sections through the modification of the  $\chi\chi g$  vertex.<sup>2</sup> We take two benchmark cases with  $\kappa = 0$  and  $\kappa = 1$  in our analysis.

### III. LHC PHENOMENOLOGY & SEARCH STRATEGY

We keep our computational setup the same as before [87]. We use `FeynRules` [94] to create the UFO [95] model files for the Lagrangians in Eqs. (14)–(16). Both the signal and the background events are generated in `MadGraph5` [96] at the leading order (LO). We include higher-order corrections to the background processes with QCD  $K$ -factors wherever available. For VLQs, higher order  $K$ -factors for signal processes are yet not known. We use NNPDF2.3LO [97] parton distribution functions (PDFs) with default dynamical renormalization and factorization scales to generate events in `MadGraph5` and then pass them through `Pythia6` [98] for showering and hadronization. Detector effects are simulated using `Delphes3` [99] with

the default CMS card. Fatjets are reconstructed from `Delphes` tower objects using Cambridge-Aachen [100] clustering algorithm (with  $R = 1.5$ ) in `FastJet` [101]. We reconstruct hadronic tops from fatjets with `HEPTopTagger` [102].

#### A. Production at the LHC

The vLQs would be produced resonantly at the LHC through the pair and the single production channels. The dominant pair production diagrams are free of the new couplings and depend only on the universal strong coupling (there are diagrams with  $t$ -channel lepton exchange that involve new couplings, but their contribution to the total pair production cross section is small [92]), hence the process is mostly model-independent up to a choice of  $\kappa$ . The pair production would lead to the following final states,

$$pp \rightarrow \left\{ \begin{array}{l} \chi_1\chi_1 \rightarrow (t\ell)(t\ell) / (t\ell)(b\nu) / (b\nu)(b\nu) \\ \chi_2\chi_2 \rightarrow (t\nu)(t\nu) / (t\nu)(b\ell) / (b\ell)(b\ell) \\ \chi_5\chi_5 \rightarrow (t\ell)(t\ell) \end{array} \right\}. \quad (18)$$

Here, as we did in case of the sLQs [87], we ignore those channels with no top quark and consider only symmetric channels i.e., both the vLQs decay to the same final state. Constraining ourselves to such channels will restrict the possible SM backgrounds and make our signal easier to detect. It is generally believed that the symmetric modes have good prospect [103].<sup>3</sup> With this considerations, we are now left with only  $(t\ell)(t\ell)$  (for  $\chi_1$  or  $\chi_5$ ) and  $(t\nu)(t\nu)$  (for  $\chi_2$ ) channels.

With similar consideration for the single production processes, where a LQ is produced in association with a lepton and either a jet or a top-quark, the possible final states are given as,

$$pp \rightarrow \left\{ \begin{array}{l} \chi_1 t\ell \rightarrow (t\ell)t\ell \\ \chi_1 \ell j \rightarrow (t\ell)\ell j \end{array} \right\}, \quad (19)$$

$$pp \rightarrow \left\{ \begin{array}{l} \chi_2 t\nu \rightarrow (t\nu)t\nu \\ \chi_2 \nu j \rightarrow (t\nu)\nu j \end{array} \right\}, \quad (20)$$

$$pp \rightarrow \left\{ \begin{array}{l} \chi_5 t\ell \rightarrow (t\ell)t\ell \\ \chi_5 \ell j \rightarrow (t\ell)\ell j \end{array} \right\}. \quad (21)$$

<sup>2</sup> Similar modifications are possible for other gauge bosons also. We, however, ignore direct electroweak  $\chi$ - $V$  couplings in our analysis.

<sup>3</sup> The asymmetric modes (where the two LQs decay differently) have not been used for LQs searches so far. For some LQ models, asymmetric channels could provide better reach than symmetric channels and, therefore, require a separate dedicated analysis [104].

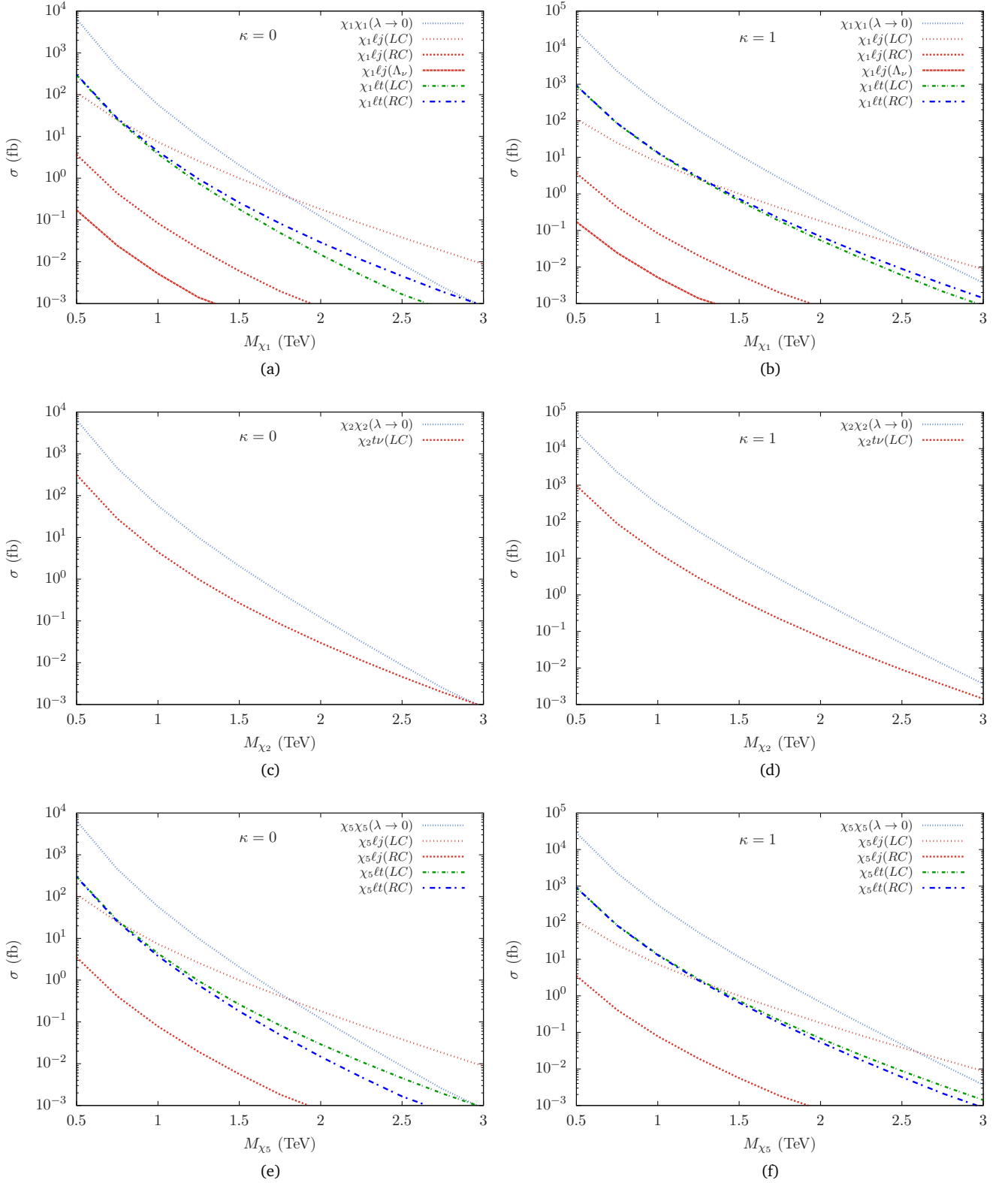


FIG. 2. The parton-level cross sections of different production channels of  $\chi_1$  [(a) and (b)],  $\chi_2$  [(c) and (d)] and  $\chi_5$  [(e) and (f)] at the 14 TeV LHC as functions of  $M_{\chi_n}$ . The single production cross sections are computed for a benchmark coupling  $\lambda = 1$  (see Table I). Here,  $\ell$  stands for either an electron or a muon and the  $j$  in the single production processes includes all the light jets as well as  $b$ -jets. Their cross sections are generated with a cut on the transverse momentum of the jet,  $p_T^j > 20$  GeV.

In Fig. 1, we show some representative Feynman diagrams of the pair and the single productions of vLQs.

In Fig. 2, we show the parton level cross sections of different production processes of  $\chi_1$  [Figs. 2(a), 2(b)],  $\chi_2$  [Figs. 2(c), 2(d)] and  $\chi_5$  [Figs. 2(e), 2(f)] as functions of their masses. The single production cross sections scale as  $\lambda^2$ . Here, they are computed for different benchmark scenarios with reference value  $\lambda = 1$ . We see that in the LC scenario with  $\kappa = 0$ , the single production cross section  $\sigma(pp \rightarrow \chi_1 \ell j)$  overtakes the pair production cross section at about 1.8 TeV while  $\sigma(pp \rightarrow \chi_1 t \ell)$  always remains smaller. For  $\kappa = 1$ , the pair production cross section increases moving the crossover point with  $\sigma(pp \rightarrow \chi_1 \ell j)$  to about 2.6 TeV. Interestingly, we find that  $\sigma(pp \rightarrow \chi_1 t \ell)$  depends on the choice of  $\kappa$  despite being a single production process as it contains  $\kappa$ -dependent  $\chi_1 \chi_1 g$  vertex. In the RC scenario,  $\sigma(pp \rightarrow \chi_1 \ell j)$  is reduced by almost two orders of magnitude than that in the LC scenario. This happens because in the RC scenario, a  $\chi_1$  couples to a right-handed top that comes from another left-handed top generated in the charged current interaction through a chirality flip. If the  $\Lambda_\nu$  coupling alone is turned on, the cross section for  $pp \rightarrow \chi_1 \ell j$  process is negligible (see in Figs. 2(a) and 2(b)). (Note, however, a nonzero  $\Lambda_\nu$  can still affect the BRs. For example, we can consider RLCSS and RLCOS scenarios where the BR for the  $\chi_1 \rightarrow t \ell$  and  $\chi_1 \rightarrow b \nu$  modes are 50% each.) Now, because of the small contribution from the  $\Lambda_\nu$  dependent diagrams and the fact that there is no interference in both the RLCSS and RLCOS scenarios, the  $pp \rightarrow \chi_1 \ell j$  process would have the same cross section as in the RC scenario. For  $\chi_2$ , pair production  $pp \rightarrow \chi_2 \chi_2$  always dominates over single production  $pp \rightarrow \chi_2 t \nu$  up to 3 TeV mass with  $\lambda = 1$  coupling for both  $\kappa = 0$  and  $\kappa = 1$ . In this case, we obtain a  $tt$  plus large  $\cancel{E}_T$  signature which is analyzed in Ref. [88]. The  $\chi_5$  vLQ is similar to the  $\chi_1$  and yield similar signatures at the colliders.

The distinctive feature of our signal is the presence of boosted top quarks and high- $p_T$  charged leptons. In symmetric modes, we have at least one top quark in the final state for single productions while the pair production give rise to two top quarks. In both the cases, we have two high- $p_T$  charged leptons. Therefore, as already indicated in the [Introduction](#), we combine events from both pair and single productions by demanding at least one top-jet (a hadronically decaying top quark forming a fatjet) and exactly two high- $p_T$  same-flavor-opposite-signs (SFOS) leptons in the final state to enhance the signal sensitivity. Note that the same final state can arise from the pair and the single productions. For example, the  $t \ell t \ell$  state can come from both  $pp \rightarrow \chi_{1,5} \chi_{1,5}$  and  $pp \rightarrow \chi_{1,5} t \ell$  processes [see Figs. 1(c) & 1(d)]. This can lead to double counting the contribution of some diagrams while generating signal events. One can bypass it by ensuring both  $\chi$  and  $\chi^\dagger$  are not on-shell simultaneously in any single production event [92].

## B. Backgrounds and selection

Since the topology of the vLQ signal is identical to that of the sLQ signal [i.e., at least one (hadronic) top fatjet and exactly two high- $p_T$  SFOS leptons], our background analysis essentially remains the same as before [87]. We therefore point the reader to the earlier paper for a detailed discussion on the possible SM background processes. Here, we present the gist of our discussions there. The dominant SM background processes for our desired signal can arise from processes having two leptons and significant cross sections at the LHC. The top-

Background processes		$\sigma$ (pb)	QCD Order
$V + jets$ [105, 106]	$Z + jets$	$6.33 \times 10^4$	NNLO
	$W + jets$	$1.95 \times 10^5$	NLO
$VV + jets$ [107]	$WW + jets$	124.31	NLO
	$WZ + jets$	51.82	NLO
	$ZZ + jets$	17.72	NLO
Single $t$ [108]	$tW$	83.1	N <sup>2</sup> LO
	$tb$	248.0	N <sup>2</sup> LO
	$tj$	12.35	N <sup>2</sup> LO
$tt$ [109]	$tt + jets$	988.57	N <sup>3</sup> LO
$ttV$ [110]	$ttZ$	1.045	NLO+NNLL
	$ttW$	0.653	NLO+NNLL

TABLE II. Total cross sections without any cut for SM background processes considered in our analysis. The higher order QCD cross sections are taken from the literature and are shown in the last column. We use these cross sections to compute the  $K$ -factors which we multiply the LO cross sections to include higher-order effects.

like fatjet can appear either from an actual top quark decaying hadronically or from a bunch of QCD/non-QCD jets mimicking its signature. We find that  $pp \rightarrow Z + jets$  and  $pp \rightarrow tt + jets$  processes contribute majorly to the background. The single top, diboson and  $ttV$  ( $V = W, Z$ ) production processes are subdominant. There are SM processes with large cross sections e.g.  $pp \rightarrow W + jets \rightarrow \ell \nu + jets$  can in principle act as backgrounds because of a jet faking as a lepton. However, we found that these processes actually contribute negligibly, thanks to a very small misidentification efficiency.

In Table II, we list the relevant SM processes and their higher-order cross sections. We consider these backgrounds after adjusting with appropriate  $K$ -factors to include higher-order effects. Although the bare cross sections (i.e. without any cut) of some background processes are seemingly huge, we control them by applying strong selection cuts. These cuts are designed in a way such that they would drastically reduce the background without harming the signal much since our signal possesses specific kinematic features very different from the backgrounds. However, some backgrounds are so big at the beginning (e.g.,  $Z + jets$ ), in order to save computation time and have better statistics, we apply the following strong cuts at the generation level.

1.  $p_T(\ell_1) > 250$  GeV,
2. Invariant mass  $M(\ell_1, \ell_2) > 115$  GeV ( $Z$ -mass veto).

Here  $\ell_i$  denotes the  $i^{\text{th}}$   $p_T$ -ordered lepton ( $e/\mu$ ). After generating events with the above generation-level cuts, we apply the following final selection criteria sequentially on the signal and the background events at the analysis level.

- $C_1$ : (a) Minimum one top-jet (obtained from HEPTopTagger) with  $p_T(t_h) > 135$  GeV.
- (b) Exactly two SFOS leptons with  $p_T(\ell_1) > 400$  GeV and  $p_T(\ell_2) > 200$  GeV and pseudorapidity  $|\eta(\ell)| < 2.5$ . For  $e$ , we consider the barrel-endcap cut on  $\eta$  between 1.37 and 1.52.
- (c) Invariant mass of the lepton pair  $M(\ell_1, \ell_2) > 120$  GeV ( $Z$ -veto).
- (d) The missing energy  $\cancel{E}_T < 200$  GeV.

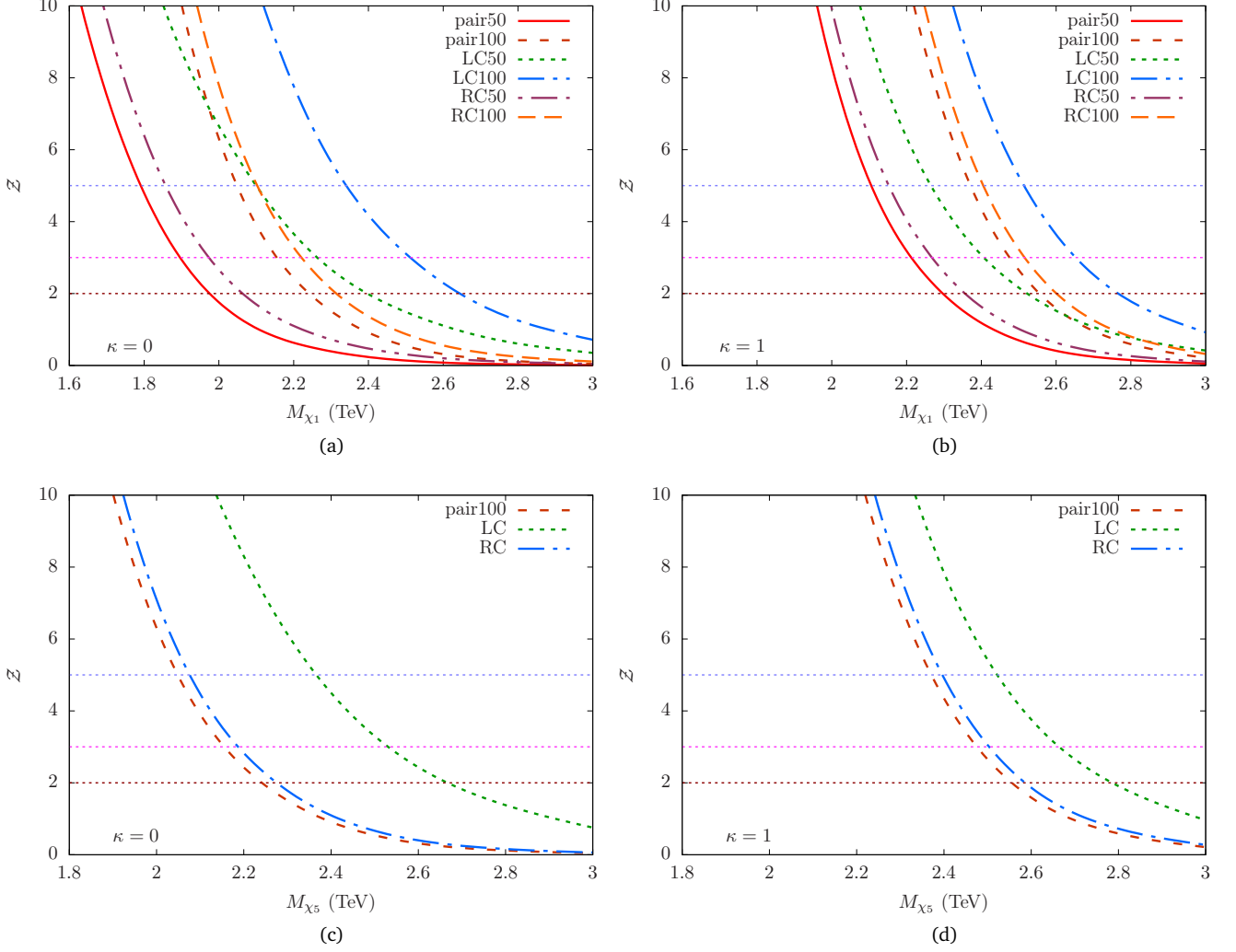


FIG. 3. Expected significance ( $\mathcal{Z}$ ) in the unit of standard deviation ( $\sigma$ ) for observing the  $\chi_1$  (a) [ $\kappa = 0$ ], (b) [ $\kappa = 1$ ] and  $\chi_5$  (c) [ $\kappa = 0$ ], (d) [ $\kappa = 1$ ] signals over the SM backgrounds. They are plotted as functions of their masses for  $3 \text{ ab}^{-1}$  of integrated luminosity at the 14 TeV HL-LHC for different coupling scenarios in the electron mode. We use the combined pair and single productions for the signals in the LC and RC scenarios. We also show the pair production significance for 50% and 100% BR in the  $\chi \rightarrow t\ell$  decay mode. We have considered  $\lambda = 1$  while computing the signals.

Significance $\mathcal{Z}$	Limit on $M_\chi$ (TeV)																	
	$\kappa = 0$									$\kappa = 1$								
	$\chi_1$				$\chi_5$					$\chi_1$				$\chi_5$				
	Combined		Pair		Combined	Pair	BR=1	Combined	Pair	BR=1	Combined		Pair		BR=1	Combined	Pair	BR=1
LC50	LC	RC50	RC	BR=0.5	BR=1	LC	RC	BR=1	LC50	LC	RC50	RC	BR=0.5	BR=1	LC	RC	BR=1	
5	2.10	2.34	1.85	2.10	1.79	2.05	2.36	2.07	2.04	2.26	2.51	2.14	2.40	2.10	2.36	2.52	2.39	2.36
3	2.25	2.51	1.97	2.22	1.89	2.15	2.52	2.18	2.15	2.40	2.65	2.26	2.51	2.21	2.47	2.66	2.50	2.47
2	2.39	2.64	2.06	2.31	1.97	2.23	2.66	2.27	2.23	2.52	2.76	2.35	2.59	2.29	2.55	2.78	2.58	2.55

TABLE III. The mass limits corresponding to  $5\sigma$  (discovery),  $3\sigma$  and  $2\sigma$  (exclusion) significances ( $\mathcal{Z}$ ) for observing the (a)  $\chi_1$  and (b)  $\chi_5$  signals over the SM backgrounds for  $3 \text{ ab}^{-1}$  integrated luminosity at the 14 TeV LHC with combined and pair-production-only signals. Here, LC (RS) stands for LC100 (RC100).

$C_2$ : The scalar sum of the transverse  $p_T$  of all visible objects,  
 $S_T > 1.2 \times \text{Min}(M_\chi, 1750) \text{ GeV}$ .

$C_3$ :  $\text{Max}(M(\ell_1, t) \text{ OR } M(\ell_2, t)) > 0.8 \times \text{Min}(M_\chi, 1750) \text{ GeV}$ .

#### IV. DISCOVERY POTENTIAL

We use the following formula to estimate the signal significance  $\mathcal{Z}$ .

$$\mathcal{Z} = \sqrt{2(N_S + N_B) \ln \left( \frac{N_S + N_B}{N_B} \right) - 2N_S}, \quad (22)$$

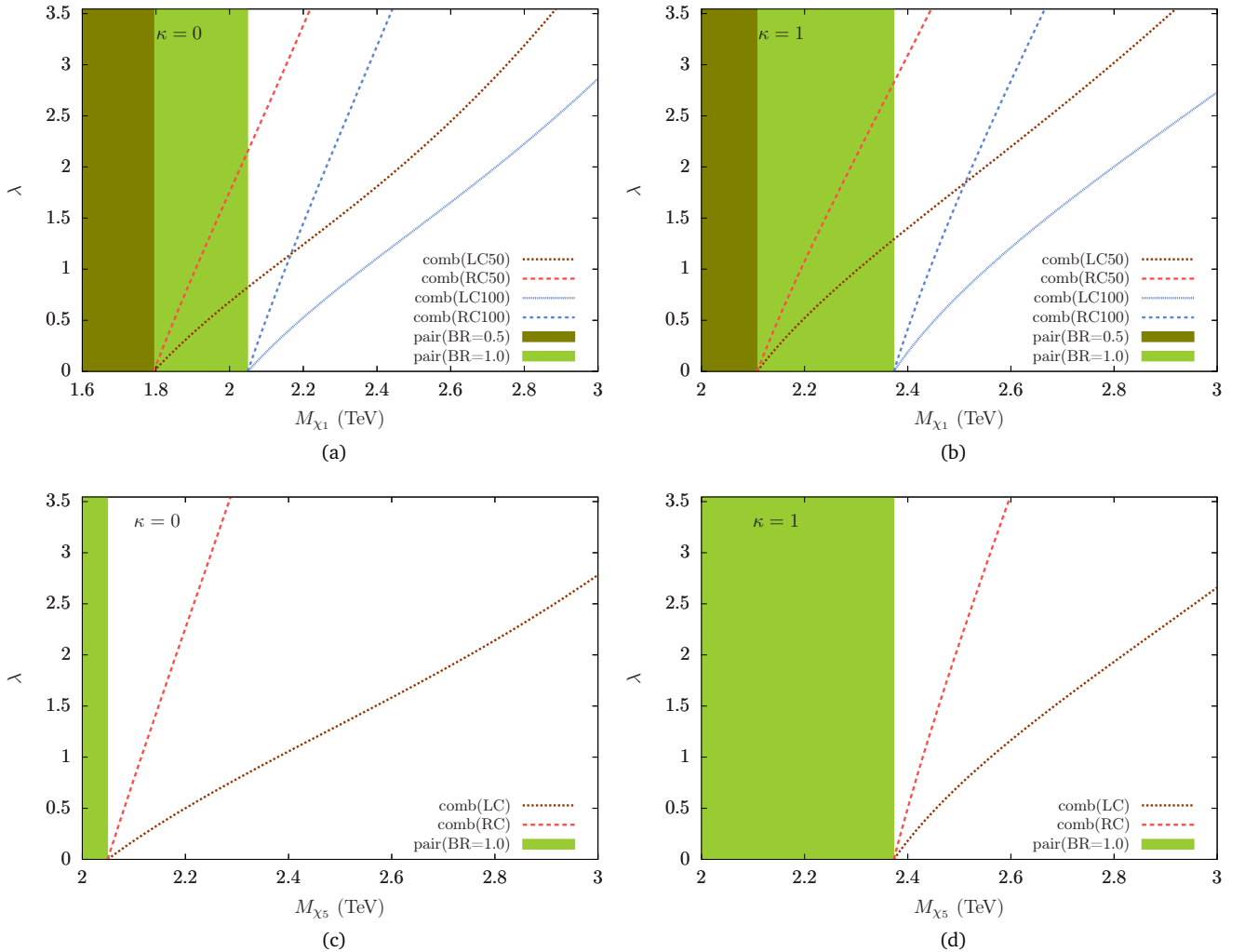


FIG. 4. The  $5\sigma$  discovery reaches in the  $\lambda$ - $M_\chi$  planes for  $\chi_1$  with (a)  $\kappa = 0$  and (b)  $\kappa = 1$  and for  $\chi_5$  with (c)  $\kappa = 0$  and (d)  $\kappa = 1$ . These plots show the smallest  $\lambda$  needed to observe  $\chi_1$  and  $\chi_5$  signals with  $5\sigma$  significance for a range of  $M_\chi$  with  $3 \text{ ab}^{-1}$  of integrated luminosity. The pair-production-only regions for 50% and 100% BRs in the  $\chi \rightarrow t\ell$  decay mode are shown with shades of green. Since the pair production is insensitive to  $\lambda$ , a small coupling is sufficient to attain  $5\sigma$  significance within the green regions.

where the number of signal and background events surviving the final selection cuts, as listed in the previous section, are denoted by  $N_S$  and  $N_B$ , respectively. In Fig. 3, we show expected significance as functions of vLQ masses. As discussed earlier, the choice of  $\kappa$  affects the pair and as well as some single productions. In Figs. 3(a) and 3(b), we present  $\mathcal{Z}$  for  $\chi_1$  with  $\kappa = 0$  and  $\kappa = 1$ , respectively. Similarly, Figs. 3(c) and 3(d) are for  $\chi_5$ . These curves are obtained for the 14 TeV LHC with  $3 \text{ ab}^{-1}$  of integrated luminosity. We have used  $\lambda = 1$  to estimate the significance for the combined signal (i.e. the pair and single production events together). We note the following points:

- The LC100 (RC100) curves for  $\chi_1$  and the LC (RC) curves for  $\chi_5$  represent the significances in the LC (RC) scenario where the BR of the  $\chi_1 \rightarrow t\ell$  decay is 100%.
- For  $\chi_1$ , the LC50 and RC50 curves represent the cases where the BR of  $\chi_1 \rightarrow t\ell$  decay mode is 50%. Although, they are not realized in the LC and RC scenarios, such a situation is possible if there are other decay modes of  $\chi_1$  (which play no role in our analysis beyond modifying the BR). Hence, we show these plots to give some estimates

of how the significance would vary with the BR.

- For comparison, we also show the expected significance obtained with only the pair production events for the 50% and 100% BR cases. For instance, for 100% BR in the  $\chi_1 \rightarrow t\ell$  mode, the HL-LHC ( $3 \text{ ab}^{-1}$ ) discovery mass reach (i.e.,  $\mathcal{Z} = 5\sigma$ ) with only pair production is about 2.05 (2.35) TeV for  $\kappa = 0$  ( $\kappa = 1$ ).
- When the LC coupling is unity, the discovery reach goes up to 2.35 (2.50) TeV once the single productions are included. However, in case of the RC scenario, the improvement is minor. This happens because  $\sigma(pp \rightarrow \chi_1 \ell j)$  is larger in the LC scenario than that in the RC scenario.
- Unlike the scalar case, there is no interference among the different signal diagrams and hence, the signal significance in the RLCSS or RLCOS benchmarks are the same as that in the RC scenario.
- In Figs. 3(c), 3(d), we observe that the maximum reach for  $\chi_5$  comes from the combined LC scenario. The values are 2.35 TeV and 2.50 TeV for  $\kappa = 0$  and  $\kappa = 1$ ,



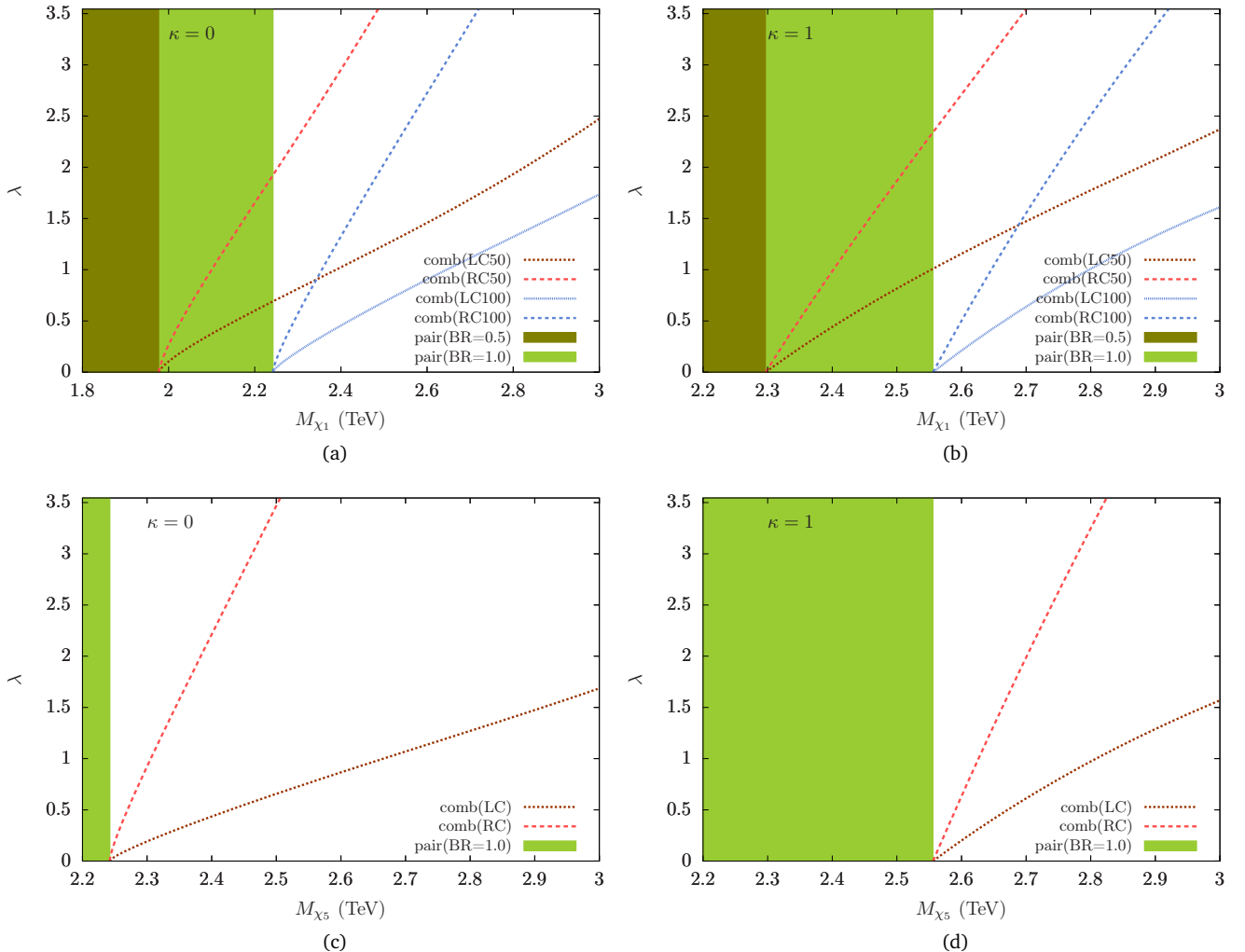


FIG. 5. The  $2\sigma$  exclusion limits in the  $\lambda$ - $M_\chi$  planes for  $\chi_1$  with (a)  $\kappa = 0$  and (b)  $\kappa = 1$  and for  $\chi_5$  with (c)  $\kappa = 0$  and (d)  $\kappa = 1$ . These plots show the smallest  $\lambda$  that can be excluded by the HL-LHC with  $3 \text{ ab}^{-1}$  of integrated luminosity. The pair-production-only regions for 50% and 100% BRs in the  $\chi \rightarrow t\ell$  decay mode are shown with green shades.

respectively. There is a suppression in the RC channel because of similar reason as for  $\chi_1$ , a  $\chi_5$  LQ also couples to a right chiral top.

In Table III we collect all the numbers for  $Z = 2\sigma, 3\sigma$  and  $5\sigma$ .

Since, we can parameterize the combined signal cross section for any  $M_\chi$  as

$$\sigma_{\text{signal}} \approx \sigma_{\text{pair}}(M_\chi) + \lambda^2 \sigma_{\text{single}}(\lambda = 1, M_\chi), \quad (23)$$

the combined signal cross section increases with  $\lambda$  for any fixed  $M_\chi$ . By recasting the figures shown in 3 which are for  $\lambda = 1$ , we can obtain the reach in the  $\lambda$ - $M_\chi$  plane, as we show in Figs. 4 and 5. We show the  $5\sigma$  discovery curves in Fig. 4 while the  $2\sigma$  exclusion curves are displayed in Fig. 5. These plots show the lowest value of  $\lambda$  required to observe the vLQ signal for a varying  $M_\chi$  with  $5\sigma$  confidence level for discovery. For the exclusion plots, all points above the curves can be excluded with 95% confidence level at the HL-LHC.

## V. SUMMARY AND CONCLUSIONS

Usually, in the direct LQ searches, it is assumed that LQs only couple to quarks and leptons of the same generation. Col-

lider signatures of TeV scale LQs with large cross-generational couplings, motivated by the persistent flavor anomalies, are completely different than what is considered in the usual LQ searches at the LHC. It is then important to explore these possibilities in detail. In a previous paper [87], we investigated the HL-LHC prospects of all scalar LQ models within the Buchmüller-Rückl-Wyler classifications [89] that would produce *boosted- $t$  + high- $p_T$ - $\ell$*  signatures at the LHC. In this follow-up paper, we investigate the case for the vector LQs with the same signature. The vLQs that decay to a top-quark can have three possible electric charges,  $\pm 1/3$ ,  $\pm 2/3$  and  $\pm 5/3$ . Among these, our primary focus is on the charge  $\pm 1/3$ ,  $\pm 5/3$  vLQs that can decay to a top quark and an electron or a muon as a unique top-lepton resonance system would appear from the decays of these LQs.

In this paper, we have introduced some simple phenomenological Lagrangians suitable for bottom-up/experimental studies. These simple models can cover the relevant parameter spaces of the full models described in listed in Refs. [89, 90]. In this simplified framework, we study the pair and single production channels of vector LQs at the LHC. Pair production of the vLQs produce final states with two boosted top quarks and two high- $p_T$  leptons and determine the LHC discovery reach

in the low mass region. Whereas, the single productions produce final state with at least one boosted top quark and two high- $p_T$  leptons. We observe two interesting points about the single productions: 1) despite considering vLQ couplings with only third generation quarks, we see that the single production cross sections are not necessarily very small, provided, of course, the new couplings controlling them are not negligible, 2) like the pair production, some single production processes can also depend on the parameter  $\kappa$  that appears in the gluon-vector LQ coupling. In some scenarios, for order one new coupling(s), the single productions would control the LHC reach in the high mass region.

We have adopted a search strategy of selecting events with at least one boosted hadronic top quark and exactly two high- $p_T$  leptons of same flavor and opposite sign. This combines events from the pair and single productions and, therefore, enhance the discovery reach by about 300 GeV from the usual pair pro-

duction searches at the LHC. Our results show that charge  $1/3$  and  $5/3$  vector LQs can be probed up to 2.35 (2.50) TeV for 100% branching ratio in the  $t\ell$  decay mode for  $\kappa = 0$  ( $\kappa = 1$ ) and order one new couplings at the 14 TeV LHC with  $3 \text{ ab}^{-1}$  of integrated luminosity with  $5\sigma$  significance. Alternately, in absence their discoveries, they can be excluded up to 2.65 (2.75) TeV at 95% confidence limit. Since the single production cross sections scale as  $\lambda^2$ , we also show how the discovery/exclusion reach would vary with  $\lambda$  within its perturbative domain.

## ACKNOWLEDGMENTS

A. B. and S.M. acknowledge support from the Science and Engineering Research Board (SERB), DST, India under grant number ECR/2017/000517.

- 
- [1] **BaBar** collaboration, J. P. Lees et al., *Evidence for an excess of  $\bar{B} \rightarrow D^{(*)}\tau^-\bar{\nu}_\tau$  decays*, *Phys. Rev. Lett.* **109** (2012) 101802, [1205.5442].
- [2] **BaBar** collaboration, J. P. Lees et al., *Measurement of an Excess of  $\bar{B} \rightarrow D^{(*)}\tau^-\bar{\nu}_\tau$  Decays and Implications for Charged Higgs Bosons*, *Phys. Rev.* **D88** (2013) 072012, [1303.0571].
- [3] **LHCb** collaboration, R. Aaij et al., *Measurement of the ratio of branching fractions  $B(\bar{B}^0 \rightarrow D^{*+}\tau^-\bar{\nu}_\tau)/B(\bar{B}^0 \rightarrow D^{*+}\mu^-\bar{\nu}_\mu)$* , *Phys. Rev. Lett.* **115** (2015) 111803, [1506.08614]. [Erratum: *Phys. Rev. Lett.* 115, no. 15, 159901 (2015)].
- [4] **LHCb** collaboration, R. Aaij et al., *Measurement of the ratio of the  $B^0 \rightarrow D^{*+}\tau^+\nu_\tau$  and  $B^0 \rightarrow D^{*+}\mu^+\nu_\mu$  branching fractions using three-prong  $\tau$ -lepton decays*, *Phys. Rev. Lett.* **120** (2018) 171802, [1708.08856].
- [5] **LHCb** collaboration, R. Aaij et al., *Test of Lepton Flavor Universality by the measurement of the  $B^0 \rightarrow D^{*+}\tau^+\nu_\tau$  branching fraction using three-prong  $\tau$  decays*, *Phys. Rev.* **D97** (2018) 072013, [1711.02505].
- [6] **Belle** collaboration, M. Huschle et al., *Measurement of the branching ratio of  $\bar{B} \rightarrow D^{(*)}\tau^-\bar{\nu}_\tau$  relative to  $\bar{B} \rightarrow D^{(*)}\ell^-\bar{\nu}_\ell$  decays with hadronic tagging at Belle*, *Phys. Rev.* **D92** (2015) 072014, [1507.03233].
- [7] **Belle** collaboration, S. Hirose et al., *Measurement of the  $\tau$  lepton polarization and  $R(D^*)$  in the decay  $\bar{B} \rightarrow D^*\tau^-\bar{\nu}_\tau$* , *Phys. Rev. Lett.* **118** (2017) 211801, [1612.00529].
- [8] **Belle** collaboration, S. Hirose et al., *Measurement of the  $\tau$  lepton polarization and  $R(D^*)$  in the decay  $\bar{B} \rightarrow D^*\tau^-\bar{\nu}_\tau$  with one-prong hadronic  $\tau$  decays at Belle*, *Phys. Rev.* **D97** (2018) 012004, [1709.00129].
- [9] **Belle** collaboration, A. Abdesselam et al., *Measurement of  $\mathcal{R}(D)$  and  $\mathcal{R}(D^*)$  with a semileptonic tagging method*, 1904.08794.
- [10] D. Bigi and P. Gambino, *Revisiting  $B \rightarrow D\ell\nu$* , *Phys. Rev.* **D94** (2016) 094008, [1606.08030].
- [11] F. U. Bernlochner, Z. Ligeti, M. Papucci and D. J. Robinson, *Combined analysis of semileptonic  $B$  decays to  $D$  and  $D^*$ :  $R(D^{(*)})$ ,  $|V_{cb}|$ , and new physics*, *Phys. Rev.* **D95** (2017) 115008, [1703.05330]. [erratum: *Phys. Rev.* D97, no. 5, 059902 (2018)].
- [12] D. Bigi, P. Gambino and S. Schacht,  *$R(D^*)$ ,  $|V_{cb}|$ , and the Heavy Quark Symmetry relations between form factors*, *JHEP* **11** (2017) 061, [1707.09509].
- [13] S. Jaiswal, S. Nandi and S. K. Patra, *Extraction of  $|V_{cb}|$  from  $B \rightarrow D^{(*)}\ell\nu_\ell$  and the Standard Model predictions of  $R(D^{(*)})$* , *JHEP* **12** (2017) 060, [1707.09977].
- [14] **LHCb** collaboration, R. Aaij et al., *Differential branching fractions and isospin asymmetries of  $B \rightarrow K^{(*)}\mu^+\mu^-$  decays*, *JHEP* **06** (2014) 133, [1403.8044].
- [15] **LHCb** collaboration, R. Aaij et al., *Test of lepton universality using  $B^+ \rightarrow K^+\ell^+\ell^-$  decays*, *Phys. Rev. Lett.* **113** (2014) 151601, [1406.6482].
- [16] **LHCb** collaboration, R. Aaij et al., *Angular analysis of the  $B^0 \rightarrow K^{*0}\mu^+\mu^-$  decay using  $3 \text{ fb}^{-1}$  of integrated luminosity*, *JHEP* **02** (2016) 104, [1512.04442].
- [17] **LHCb** collaboration, R. Aaij et al., *Test of lepton universality with  $B^0 \rightarrow K^{*0}\ell^+\ell^-$  decays*, *JHEP* **08** (2017) 055, [1705.05802].
- [18] **LHCb** collaboration, R. Aaij et al., *Search for lepton-universality violation in  $B^+ \rightarrow K^+\ell^+\ell^-$  decays*, *Phys. Rev. Lett.* **122** (2019) 191801, [1903.09252].
- [19] G. Hiller and F. Kruger, *More model-independent analysis of  $b \rightarrow s$  processes*, *Phys. Rev.* **D69** (2004) 074020, [hep-ph/0310219].
- [20] M. Bordone, G. Isidori and A. Pattori, *On the Standard Model predictions for  $R_K$  and  $R_{K^*}$* , *Eur. Phys. J.* **C76** (2016) 440, [1605.07633].
- [21] **LHCb** collaboration, R. Aaij et al., *Measurement of the ratio of branching fractions  $B(B_c^+ \rightarrow J/\psi\tau^+\nu_\tau)/B(B_c^+ \rightarrow J/\psi\mu^+\nu_\mu)$* , *Phys. Rev. Lett.* **120** (2018) 121801, [1711.05623].
- [22] **Muon g-2** collaboration, G. W. Bennett et al., *Final Report of the Muon E821 Anomalous Magnetic Moment Measurement at BNL*, *Phys. Rev.* **D73** (2006) 072003, [hep-ex/0602035].
- [23] Y. Sakaki, M. Tanaka, A. Tayduganov and R. Watanabe, *Testing leptoquark models in  $\bar{B} \rightarrow D^{(*)}\tau\bar{\nu}$* , *Phys. Rev. D* **88** (2013) 094012, [1309.0301].
- [24] R. Mohanta, *Effect of scalar leptoquarks on the rare decays of  $B_s$  meson*, *Phys. Rev.* **D89** (2014) 014020, [1310.0713].
- [25] S. Sahoo and R. Mohanta, *Scalar leptoquarks and the rare  $B$  meson decays*, *Phys. Rev.* **D91** (2015) 094019, [1501.05193].

- [26] U. K. Dey and S. Mohanty, *Constraints on Leptoquark Models from IceCube Data*, *JHEP* **04** (2016) 187, [[1505.01037](#)].
- [27] T. Mandal, S. Mitra and S. Seth, *Pair Production of Scalar Leptoquarks at the LHC to NLO Parton Shower Accuracy*, *Phys. Rev. D* **93** (2016) 035018, [[1506.07369](#)].
- [28] M. Freytsis, Z. Ligeti and J. T. Ruderman, *Flavor models for  $\bar{B} \rightarrow D^{(*)} \tau \bar{\nu}$* , *Phys. Rev. D* **92** (2015) 054018, [[1506.08896](#)].
- [29] S. Sahoo and R. Mohanta, *Study of the rare semileptonic decays  $B_d^0 \rightarrow K^* l^+ l^-$  in scalar leptoquark model*, *Phys. Rev. D* **93** (2016) 034018, [[1507.02070](#)].
- [30] S. Sahoo and R. Mohanta, *Leptoquark effects on  $b \rightarrow s \nu \bar{\nu}$  and  $B \rightarrow Kl^+ l^-$  decay processes*, *New J. Phys.* **18** (2016) 013032, [[1509.06248](#)].
- [31] U. Aydemir, *SO(10) grand unification in light of recent LHC searches and colored scalars at the TeV-scale*, *Int. J. Mod. Phys. A* **31** (2016) 1650034, [[1512.00568](#)].
- [32] S. Sahoo and R. Mohanta, *Lepton flavor violating B meson decays via a scalar leptoquark*, *Phys. Rev. D* **93** (2016) 114001, [[1512.04657](#)].
- [33] U. Aydemir and T. Mandal, *LHC probes of TeV-scale scalars in SO(10) grand unification*, *Adv. High Energy Phys.* **2017** (2017) 7498795, [[1601.06761](#)].
- [34] D. Das, C. Hati, G. Kumar and N. Mahajan, *Towards a unified explanation of  $R_{D^{(*)}}$ ,  $R_K$  and  $(g-2)_\mu$  anomalies in a left-right model with leptoquarks*, *Phys. Rev. D* **94** (2016) 055034, [[1605.06313](#)].
- [35] S. Sahoo and R. Mohanta, *Effects of scalar leptoquark on semileptonic  $\Lambda_b$  decays*, *New J. Phys.* **18** (2016) 093051, [[1607.04449](#)].
- [36] D. Bečirević, N. Košnik, O. Sumensari and R. Zukanovich Funchal, *Palatable Leptoquark Scenarios for Lepton Flavor Violation in Exclusive  $b \rightarrow s \ell_1 \ell_2$  modes*, *JHEP* **11** (2016) 035, [[1608.07583](#)].
- [37] P. Bandyopadhyay and R. Mandal, *Vacuum stability in an extended standard model with a leptoquark*, *Phys. Rev. D* **95** (2017) 035007, [[1609.03561](#)].
- [38] S. Sahoo, R. Mohanta and A. K. Giri, *Explaining the  $R_K$  and  $R_{D^{(*)}}$  anomalies with vector leptoquarks*, *Phys. Rev. D* **95** (2017) 035027, [[1609.04367](#)].
- [39] D. A. Faroughy, A. Greljo and J. F. Kamenik, *Confronting lepton flavor universality violation in B decays with high- $p_T$  tau lepton searches at LHC*, *Phys. Lett. B* **764** (2017) 126–134, [[1609.07138](#)].
- [40] G. Hiller, D. Loose and K. Schönwald, *Leptoquark Flavor Patterns & B Decay Anomalies*, *JHEP* **12** (2016) 027, [[1609.08895](#)].
- [41] B. Bhattacharya, A. Datta, J.-P. Guévin, D. London and R. Watanabe, *Simultaneous Explanation of the  $R_K$  and  $R_{D^{(*)}}$  Puzzles: a Model Analysis*, *JHEP* **01** (2017) 015, [[1609.09078](#)].
- [42] M. Duraisamy, S. Sahoo and R. Mohanta, *Rare semileptonic  $B \rightarrow K(\pi) l_i^- l_j^+$  decay in a vector leptoquark model*, *Phys. Rev. D* **95** (2017) 035022, [[1610.00902](#)].
- [43] D. Das, K. Ghosh, M. Mitra and S. Mondal, *Probing sterile neutrinos in the framework of inverse seesaw mechanism through leptoquark productions*, *Phys. Rev. D* **97** (2018) 015024, [[1708.06206](#)].
- [44] N. Assad, B. Fornal and B. Grinstein, *Baryon Number and Lepton Universality Violation in Leptoquark and Diquark Models*, *Phys. Lett. B* **777** (2018) 324–331, [[1708.06350](#)].
- [45] U. K. Dey, D. Kar, M. Mitra, M. Spannowsky and A. C. Vincent, *Searching for Leptoquarks at IceCube and the LHC*, *Phys. Rev. D* **98** (2018) 035014, [[1709.02009](#)].
- [46] A. Biswas, D. K. Ghosh, S. K. Patra and A. Shaw,  *$b \rightarrow c l \nu$  anomalies in light of extended scalar sectors*, *Int. J. Mod. Phys. A* **34** (2019) 1950112, [[1801.03375](#)].
- [47] P. Bandyopadhyay and R. Mandal, *Revisiting scalar leptoquark at the LHC*, *Eur. Phys. J. C* **78** (2018) 491, [[1801.04253](#)].
- [48] U. Aydemir, D. Minic, C. Sun and T. Takeuchi, *B-decay anomalies and scalar leptoquarks in unified Pati-Salam models from noncommutative geometry*, *JHEP* **09** (2018) 117, [[1804.05844](#)].
- [49] J. Kumar, D. London and R. Watanabe, *Combined Explanations of the  $b \rightarrow s \mu^+ \mu^-$  and  $b \rightarrow c \tau^- \bar{\nu}$  Anomalies: a General Model Analysis*, *Phys. Rev. D* **99** (2019) 015007, [[1806.07403](#)].
- [50] A. Angelescu, D. Bečirević, D. Faroughy and O. Sumensari, *Closing the window on single leptoquark solutions to the B-physics anomalies*, *JHEP* **10** (2018) 183, [[1808.08179](#)].
- [51] T. Mandal, S. Mitra and S. Raz,  *$R_{D^{(*)}}$  motivated  $S_1$  leptoquark scenarios: Impact of interference on the exclusion limits from LHC data*, *Phys. Rev. D* **99** (2019) 055028, [[1811.03561](#)].
- [52] S. Iguro, T. Kitahara, Y. Omura, R. Watanabe and K. Yamamoto,  *$D^*$  polarization vs.  $R_{D^{(*)}}$  anomalies in the leptoquark models*, *JHEP* **02** (2019) 194, [[1811.08899](#)].
- [53] J. Aebischer, A. Crivellin and C. Greub, *QCD improved matching for semileptonic B decays with leptoquarks*, *Phys. Rev. D* **99** (2019) 055002, [[1811.08907](#)].
- [54] S. Bar-Shalom, J. Cohen, A. Soni and J. Wudka, *Phenomenology of TeV-scale scalar Leptoquarks in the EFT*, *Phys. Rev. D* **100** (2019) 055020, [[1812.03178](#)].
- [55] T. J. Kim, P. Ko, J. Li, J. Park and P. Wu, *Correlation between  $R_{D^{(*)}}$  and top quark FCNC decays in leptoquark models*, *JHEP* **07** (2019) 025, [[1812.08484](#)].
- [56] S. Mandal, M. Mitra and N. Sinha, *Probing leptoquarks and heavy neutrinos at the LHeC*, *Phys. Rev. D* **98** (2018) 095004, [[1807.06455](#)].
- [57] A. Biswas, D. Kumar Ghosh, N. Ghosh, A. Shaw and A. K. Swain, *Collider signature of  $U_1$  Leptoquark and constraints from  $b \rightarrow c$  observables*, *J. Phys.* **G47** (2020) 045005, [[1808.04169](#)].
- [58] R. Mandal, *Fermionic dark matter in leptoquark portal*, *Eur. Phys. J. C* **78** (2018) 726, [[1808.07844](#)].
- [59] A. Biswas, A. Shaw and A. K. Swain, *Collider signature of  $V_2$  Leptoquark with  $b \rightarrow s$  flavour observables*, *LHEP* **2** (2019) 126, [[1811.08887](#)].
- [60] J. Roy, *Probing leptoquark chirality via top polarization at the Colliders*, [1811.12058](#).
- [61] S. Sahoo and R. Mohanta, *Impact of vector leptoquark on  $\bar{B} \rightarrow \bar{K}^* l^+ l^-$  anomalies*, *J. Phys.* **G45** (2018) 085003, [[1806.01048](#)].
- [62] A. Crivellin, C. Greub, D. Müller and F. Saturnino, *Importance of Loop Effects in Explaining the Accumulated Evidence for New Physics in B Decays with a Vector Leptoquark*, *Phys. Rev. Lett.* **122** (2019) 011805, [[1807.02068](#)].
- [63] S. Balaji, R. Foot and M. A. Schmidt, *Chiral SU(4) explanation of the  $b \rightarrow s$  anomalies*, *Phys. Rev. D* **99** (2019) 015029, [[1809.07562](#)].
- [64] B. Fornal, S. A. Gadam and B. Grinstein, *Left-Right SU(4) Vector Leptoquark Model for Flavor Anomalies*,

- Phys. Rev. D* **99** (2019) 055025, [1812.01603].
- [65] E. Alvarez and M. Szewc, *Nonresonant leptoquark with multigeneration couplings for  $\mu\mu jj$  and  $\mu\nu jj$  at the LHC*, *Phys. Rev. D* **99** (2019) 095004, [1811.05944].
- [66] R. Mandal and A. Pich, *Constraints on scalar leptoquarks from lepton and kaon physics*, *JHEP* **12** (2019) 089, [1908.11155].
- [67] W.-S. Hou, T. Modak and G.-G. Wong, *Scalar leptoquark effects on  $B \rightarrow \mu\bar{\nu}$  decay*, *Eur. Phys. J. C* **79** (2019) 964, [1909.00403].
- [68] R. Padhan, S. Mandal, M. Mitra and N. Sinha, *Signatures of  $\tilde{R}_2$  class of Leptoquarks at the upcoming ep colliders*, 1912.07236.
- [69] U. Aydemir, T. Mandal and S. Mitra, *Addressing the  $R_{D^{(*)}}$  anomalies with an  $S_1$  leptoquark from SO(10) grand unification*, *Phys. Rev. D* **101** (2020) 015011, [1902.08108].
- [70] B. Allanach, T. Corbett and M. Madigan, *Sensitivity of Future Hadron Colliders to Leptoquark Pair Production in the Di-Muon Di-Jets Channel*, *Eur. Phys. J. C* **80** (2020) 170, [1911.04455].
- [71] J. Zhang, C.-X. Yue, C.-H. Li and S. Yang, *Constraints on scalar and vector leptoquarks from the LHC Higgs data*, 1905.04074.
- [72] C. Cornella, J. Fuentes-Martin and G. Isidori, *Revisiting the vector leptoquark explanation of the B-physics anomalies*, *JHEP* **07** (2019) 168, [1903.11517].
- [73] M. J. Baker, J. Fuentes-Martin, G. Isidori and M. König, *High- $p_T$  signatures in vector-leptoquark models*, *Eur. Phys. J. C* **79** (2019) 334, [1901.10480].
- [74] A. Bhaskar, D. Das, B. De and S. Mitra, *Enhancement of Higgs Production Through Leptoquarks at the LHC*, 2002.12571.
- [75] P. Bandyopadhyay, S. Dutta and A. Karan, *Investigating the Production of Leptoquarks by Means of Zeros of Amplitude at Photon Electron Collider*, 2003.11751.
- [76] J. C. Pati and A. Salam, *Lepton Number as the Fourth Color*, *Phys. Rev. D* **10** (1974) 275–289. [Erratum: *Phys. Rev. D* **11**, 703(1975)].
- [77] H. Georgi and S. L. Glashow, *Unity of All Elementary Particle Forces*, *Phys. Rev. Lett.* **32** (1974) 438–441.
- [78] B. Schrempp and F. Schrempp, *Light Leptoquarks*, *Phys. Lett.* **B153** (1985) 101–107.
- [79] R. Barbier et al., *R-parity violating supersymmetry*, *Phys. Rept.* **420** (2005) 1–202, [hep-ph/0406039].
- [80] M. Kohda, H. Sugiyama and K. Tsumura, *Lepton number violation at the LHC with leptoquark and diquark*, *Phys. Lett.* **B718** (2013) 1436–1440, [1210.5622].
- [81] ATLAS collaboration, M. Aaboud et al., *Searches for scalar leptoquarks and differential cross-section measurements in dilepton-dijet events in proton-proton collisions at a centre-of-mass energy of  $\sqrt{s} = 13$  TeV with the ATLAS experiment*, *Eur. Phys. J. C* **79** (2019) 733, [1902.00377].
- [82] ATLAS collaboration, M. Aaboud et al., *Searches for third-generation scalar leptoquarks in  $\sqrt{s} = 13$  TeV pp collisions with the ATLAS detector*, *JHEP* **06** (2019) 144, [1902.08103].
- [83] CMS collaboration, A. M. Sirunyan et al., *Search for third-generation scalar leptoquarks decaying to a top quark and a  $\tau$  lepton at  $\sqrt{s} = 13$  TeV*, *Eur. Phys. J. C* **78** (2018) 707, [1803.02864].
- [84] CMS collaboration, A. M. Sirunyan et al., *Constraints on models of scalar and vector leptoquarks decaying to a quark and a neutrino at  $\sqrt{s} = 13$  TeV*, *Phys. Rev. D* **98** (2018) 032005, [1805.10228].
- [85] CMS collaboration, A. M. Sirunyan et al., *Search for leptoquarks coupled to third-generation quarks in proton-proton collisions at  $\sqrt{s} = 13$  TeV*, *Phys. Rev. Lett.* **121** (2018) 241802, [1809.05558].
- [86] CMS collaboration, *Projection of searches for pair production of scalar leptoquarks decaying to a top quark and a charged lepton at the HL-LHC*, Tech. Rep. CMS-PAS-FTR-18-008, 2018.
- [87] K. Chandak, T. Mandal and S. Mitra, *Hunting for scalar leptoquarks with boosted tops and light leptons*, *Phys. Rev. D* **100** (2019) 075019, [1907.11194].
- [88] N. Vignaroli, *Seeking leptoquarks in the  $t\bar{t}$  plus missing energy channel at the high-luminosity LHC*, *Phys. Rev. D* **99** (2019) 035021, [1808.10309].
- [89] W. Buchmuller, R. Ruckl and D. Wyler, *Leptoquarks in Lepton - Quark Collisions*, *Phys. Lett.* **B191** (1987) 442–448. [Erratum: *Phys. Lett.* **B448**, 320(1999)].
- [90] I. Doršner, S. Fajfer, A. Greljo, J. F. Kamenik and N. Košnik, *Physics of leptoquarks in precision experiments and at particle colliders*, *Phys. Rept.* **641** (2016) 1–68, [1603.04993].
- [91] T. Mandal and S. Mitra, *Probing Color Octet Electrons at the LHC*, *Phys. Rev. D* **87** (2013) 095008, [1211.6394].
- [92] T. Mandal, S. Mitra and S. Seth, *Single Productions of Colored Particles at the LHC: An Example with Scalar Leptoquarks*, *JHEP* **07** (2015) 028, [1503.04689].
- [93] T. Mandal, S. Mitra and S. Seth, *Probing Compositeness with the CMS  $eejj$  &  $eej$  Data*, *Phys. Lett.* **B758** (2016) 219–225, [1602.01273].
- [94] A. Alloul, N. D. Christensen, C. Degrande, C. Duhr and B. Fuks, *FeynRules 2.0 - A complete toolbox for tree-level phenomenology*, *Comput. Phys. Commun.* **185** (2014) 2250–2300, [1310.1921].
- [95] C. Degrande, C. Duhr, B. Fuks, D. Grellscheid, O. Mattelaer and T. Reiter, *UFO - The Universal FeynRules Output*, *Comput. Phys. Commun.* **183** (2012) 1201–1214, [1108.2040].
- [96] J. Alwall, R. Frederix, S. Frixione, V. Hirschi, F. Maltoni, O. Mattelaer et al., *The automated computation of tree-level and next-to-leading order differential cross sections, and their matching to parton shower simulations*, *JHEP* **07** (2014) 079, [1405.0301].
- [97] R. D. Ball et al., *Parton distributions with LHC data*, *Nucl. Phys.* **B867** (2013) 244–289, [1207.1303].
- [98] T. Sjostrand, S. Mrenna and P. Z. Skands, *PYTHIA 6.4 Physics and Manual*, *JHEP* **05** (2006) 026, [hep-ph/0603175].
- [99] DELPHES 3 collaboration, J. de Favereau, C. Delaere, P. Demin, A. Giammanco, V. Lemaître, A. Mertens et al., *DELPHES 3, A modular framework for fast simulation of a generic collider experiment*, *JHEP* **02** (2014) 057, [1307.6346].
- [100] Y. L. Dokshitzer, G. D. Leder, S. Moretti and B. R. Webber, *Better jet clustering algorithms*, *JHEP* **08** (1997) 001, [hep-ph/9707323].
- [101] M. Cacciari, G. P. Salam and G. Soyez, *FastJet User Manual*, *Eur. Phys. J. C* **72** (2012) 1896, [1111.6097].
- [102] T. Plehn, M. Spannowsky, M. Takeuchi and D. Zerwas, *Stop Reconstruction with Tagged Tops*, *JHEP* **10** (2010) 078, [1006.2833].
- [103] B. Diaz, M. Schmaltz and Y.-M. Zhong, *The leptoquark Hunter's guide: Pair production*, *JHEP* **10** (2017) 097, [1706.05033].

- [104] A. Bhaskar, T. Mandal, S. Mitra and C. Neeraj, *In preparation* .
- [105] S. Catani, L. Cieri, G. Ferrera, D. de Florian and M. Grazzini, *Vector boson production at hadron colliders: a fully exclusive QCD calculation at NNLO*, *Phys. Rev. Lett.* **103** (2009) 082001, [[0903.2120](#)].
- [106] G. Balossini, G. Montagna, C. M. Carloni Calame, M. Moretti, O. Nicrosini, F. Piccinini et al., *Combination of electroweak and QCD corrections to single W production at the Fermilab Tevatron and the CERN LHC*, *JHEP* **01** (2010) 013, [[0907.0276](#)].
- [107] J. M. Campbell, R. K. Ellis and C. Williams, *Vector boson pair production at the LHC*, *JHEP* **07** (2011) 018, [[1105.0020](#)].
- [108] N. Kidonakis, *Theoretical results for electroweak-boson and single-top production*, *PoS DIS2015* (2015) 170, [[1506.04072](#)].
- [109] C. Muselli, M. Bonvini, S. Forte, S. Marzani and G. Ridolfi, *Top Quark Pair Production beyond NNLO*, *JHEP* **08** (2015) 076, [[1505.02006](#)].
- [110] A. Kulesza, L. Motyka, D. Schwartländer, T. Stebel and V. Theeuwes, *Associated production of a top quark pair with a heavy electroweak gauge boson at NLO+NNLL accuracy*, *Eur. Phys. J.* **C79** (2019) 249, [[1812.08622](#)].